

## Optical Spectrum of Divalent Vanadium in Octahedral Coordination

M. D. STURGE

*Bell Telephone Laboratories, Murray Hill, New Jersey*

(Received 3 December 1962)

Sharp-line fluorescence of the  $V^{2+}$  ion in magnesium oxide and corundum has been studied at low temperatures, with and without a magnetic field. The excitation spectrum is used to determine the energy level scheme. The results are analyzed in terms of crystal field theory, and the vibrational structure is briefly discussed. The variation of the crystal field parameters through the  $d^3$  sequence  $V^{2+}$ ,  $Cr^{3+}$ ,  $Mn^{4+}$  is considered in terms of a point-charge model.

### 1. INTRODUCTION

THE optical spectrum of the trivalent chromium ion in octahedral and near octahedral coordination has been studied in great detail, particularly in ruby.<sup>1-4</sup> The crystal field theory has been shown to fit the results qualitatively, but in order to obtain a quantitative fit it is necessary to introduce a rather large number of variable parameters into the theory.<sup>5-7</sup>  $Cr^{3+}$  has two isoelectronic neighbors  $V^{2+}$  and  $Mn^{4+}$ , a study of which might cast light on the choice of these parameters. The spectrum of  $Mn^{4+}$  in corundum has already been reported<sup>8</sup> as has the spin resonance of  $V^{2+}$  in magnesium oxide<sup>9</sup> and corundum.<sup>10</sup> Absorption by  $V^{2+}$  in crystals at present available is too weak to be observed, as  $V^{3+}$  always seems to predominate. However, the discovery of sharp-line fluorescence due to  $V^{2+}$  in magnesium oxide<sup>11</sup> and in irradiated vanadium corundum, which has been shown to arise from the  ${}^2E \rightarrow {}^4A_2$  transition of  $V^{2+}$  (the initial and final states being degenerate in the cubic magnesium oxide but split in trigonal corundum), has made it possible to find out a great deal about the energy levels in these two crystals from the excitation spectra and Zeeman effect.

### 2. EXPERIMENTAL

Magnesium oxide single crystals doped with nominally 0.1% vanadium were obtained from the Norton Company of Canada; corundum boules grown by flame fusion and doped with similar amounts of vanadium were obtained from the Linde Company; some of the latter were additionally doped with tin or titanium in the hope of encouraging the formation of divalent vanadium. As delivered, the magnesium oxide fluoresced

weakly at  $11\,498\text{ cm}^{-1}$ . Heating in hydrogen at  $1200^\circ\text{C}$  for 5 h increased the fluorescence by two orders of magnitude. The spin resonance signal due to  $V^{2+}$  increased in the same proportion as the fluorescent intensity (within a factor of 2). Although the spin resonance indicated that after heat treatment the majority of the vanadium was in the  $V^{2+}$  state, the absorption due to  $V^{3+}$  still largely obscured that due to  $V^{2+}$  (see Fig. 6). As delivered, vanadium corundum showed no fluorescence, regardless of doping. After 14 h irradiation in a  $Co^{60}$   $\gamma$ -ray cell<sup>10</sup> (dose rate 0.7 MR/h) sharp fluorescent lines were observed at  $11\,679.2\text{ cm}^{-1}$  and  $11\,691.5\text{ cm}^{-1}$ , at  $77^\circ\text{K}$ . No absorption in this spectral region was observed, even after 14 days irradiation.

Sharp-line fluorescence was studied with a Jarrell-Ash 1.8-m Ebert scanning spectrometer,<sup>12</sup> using a spectral slit width between 0.05 and  $0.5\text{ cm}^{-1}$  according to the signal available. The detector was an RCA 7102 photomultiplier, cooled to  $77^\circ\text{K}$ . For Zeeman studies, fields up to 23.5 kG were available from a 6-in. Varian magnet. Fluorescence was excited with one or more 150-W tungsten projector lamps, or with a 1000-W mercury arc, the exciting light being filtered with dilute copper sulphate solution. Excitation spectra were taken by illuminating the specimen (normally held at  $77^\circ\text{K}$ ) with light from a Bausch & Lomb  $f/4.5$  grating monochromator, with a spectral slit width of  $40\text{--}60\text{ cm}^{-1}$ , and selecting the fluorescent light with an interference filter. When the exciting wavelength was close to the fluorescing line, it was necessary to use the Jarrell-Ash spectrometer to discriminate between the fluorescence and scattered exciting light. This reduced the signal substantially and the method could not be used for the weak fluorescence obtained from corundum.

Absorption spectra were taken on a Cary model 14 spectrophotometer. Attempts to see sharp line absorption in these specimens using the Jarrell-Ash spectrometer were unsuccessful.

### 3. RESULTS

#### A. Fluorescent Spectra and Zeeman Effect in Magnesium Oxide

In a good crystal of magnesium oxide containing about 0.005%  $V^{2+}$ , a single fluorescent line is observed

<sup>1</sup> O. Deutschbein, *Ann. Physik* **14**, 712 (1932).  
<sup>2</sup> S. Sugano and I. Tsujikawa, *J. Phys. Soc. Japan* **13**, 899 (1958).  
<sup>3</sup> S. Sugano, A. L. Schawlow, and F. Varsanyi, *Phys. Rev.* **120**, 2045 (1960).  
<sup>4</sup> D. S. McClure, in *Solid State Physics*, edited by F. Seitz and D. Turnbull (Academic Press Inc., New York, 1959), Vol. 9, p. 399 (who gives many other references).  
<sup>5</sup> Y. Tanabe and S. Sugano, *J. Phys. Soc. Japan* **9**, 766 (1954).  
<sup>6</sup> S. Sugano and Y. Tanabe, *J. Phys. Soc. Japan* **13**, 880 (1958).  
<sup>7</sup> S. Sugano and M. Peter, *Phys. Rev.* **122**, 381 (1961).  
<sup>8</sup> S. Geschwind, P. Kisliuk, M. P. Klein, J. P. Remeika, and D. L. Wood, *Phys. Rev.* **126**, 1684 (1962).  
<sup>9</sup> W. Low, *Phys. Rev.* **101**, 1827 (1956).  
<sup>10</sup> J. Lambe and C. Kikuchi, *Phys. Rev.* **118**, 71 (1960).  
<sup>11</sup> G. E. Devlin, J. A. Ditzenberger, and M. D. Sturge, *Bull. Am. Phys. Soc.* **7**, 258 (1962).

<sup>12</sup> W. G. Fastie, H. M. Crosswhite, and P. Gloerson, *J. Opt. Soc. Am.* **48**, 106 (1958).

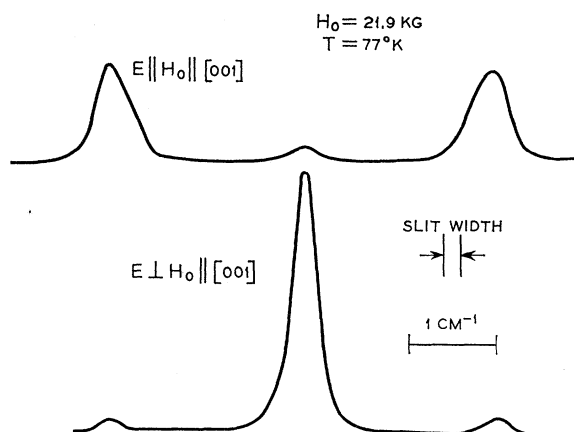


FIG. 1. Zeeman effect of the 11 498  $\text{cm}^{-1}$  fluorescence of  $\text{MgO}:\text{V}^{2+}$  (Conc.  $\text{V}^{2+} \sim 0.01\%$ ) at 77°K.

at 11 498.6  $\text{cm}^{-1}$ , 0.3  $\text{cm}^{-1}$  wide at 77°K. At room temperature the line is at 11 486  $\text{cm}^{-1}$  and about 10  $\text{cm}^{-1}$  wide. In a magnetic field the line splits into a triplet, shown for two polarizations in Fig. 1. The central component is as narrow as the zero-field line, but the outer components are broadened by an amount varying from specimen to specimen. I am unable to account for this broadening, which is not due to inhomogeneity of the magnetic field. The apparent  $g$  value at the peaks is  $2.03 \pm 0.02$ ; taking the  $g$  value in the ground state to be 1.98<sup>9</sup> and identifying the peaks with the transitions  ${}^2E(+1/2) \rightarrow {}^4A_2(+3/2)$  and  ${}^2E(-1/2) \rightarrow {}^4A_2(-3/2)$  (see Fig. 2) which are the strongest, we find  $g$  for the upper state to be  $1.88 \pm 0.04$ . The intensities of the components at 1.7°K show the effect of thermalization in the upper state, demonstrating that the upper state is a doublet, and supporting the assignment  ${}^2E \rightarrow {}^4A_2$  for this transition.

The  $g$  value is independent of the orientation of the magnetic field relative to the crystal axes, confirming that the site is cubic, but the intensities of the components vary as shown in Fig. 2. The length of each line represents its observed relative intensity, and the associated number is the predicted intensity calculated on the assumption of pure magnetic dipole transitions.<sup>3</sup> I believe the small amount of "forbidden" polarization observed in these experiments to be genuine and not due to experimental error. It can be accounted for by assuming that about 10% of the line intensity is contributed by electric dipole transitions, induced either by odd vibrations or by odd crystal fields produced by neighboring impurities or defects (in the present context  $\text{V}^{3+}$  counts as an impurity).

In the more concentrated specimens produced by heat treatment, which contain about 0.1%  $\text{V}^{2+}$ , additional structure is seen in fluorescence (Fig. 3). The sharp lines are attributed to various possible combinations of  $\text{V}^{2+}$  with other impurities and defects and will be discussed in a separate paper. The broad peaks are

vibrational satellites, involving the emission of a phonon. The main peaks are at 270 and 490  $\text{cm}^{-1}$  from the main line, with weaker maxima at 420 and 540  $\text{cm}^{-1}$ . These separations agree very closely with those observed in the corresponding spectrum of  $\text{Cr}^{3+}$ .<sup>1</sup> At 300°K weak fluorescence is seen on the high-frequency side of the line, with maxima at 260, 410, and 490  $\text{cm}^{-1}$  above the pure electronic line.

Even in the most concentrated samples no sharp line absorption is observed in the region of 11 500  $\text{cm}^{-1}$ , the limit of observation being 0.03  $\text{cm}^{-1}$ . This puts an upper limit on the oscillator strength for the  ${}^4A_2 \rightarrow {}^2E$  transition of  $2 \times 10^{-9}$  (taking the concentration of  $\text{V}^{2+}$  to be at least 0.05%). The oscillator strength calculated on the assumption of pure magnetic dipole transitions<sup>3</sup> using the parameters determined in Sec. 4 is  $2 \times 10^{-9}$ . The fluorescent lifetime was measured roughly by watching the decay of fluorescence after flash excitation. It is about 50 msec at 77°K and 25 msec at 300°K. This is presumably limited by nonradiative processes, as the radiative lifetime calculated from  $f = 2 \times 10^{-9}$  is one second.

## B. Fluorescent Spectra and Zeeman Effect in Corundum

In the best crystals of vanadium corundum, extremely sharp lines, about 0.10  $\text{cm}^{-1}$  wide at 4.2°K, were observed after 14-h irradiation. Figure 4 shows the  $\sigma$ -polarized fluorescence observed in zero field and with a magnetic field  $H_0$  parallel to the  $C_3$  axis. The "R1" line ( $\bar{E} \rightarrow {}^4A_2$ ) is shown at 4.2°K; the "R1" ( $2\bar{A} \rightarrow {}^4A_2$ ) is not visible at 4.2°K because of the depopulation of the  $2\bar{A}$  state (which is in thermal equilibrium with the  $\bar{E}$  state) and is shown at 77°K.

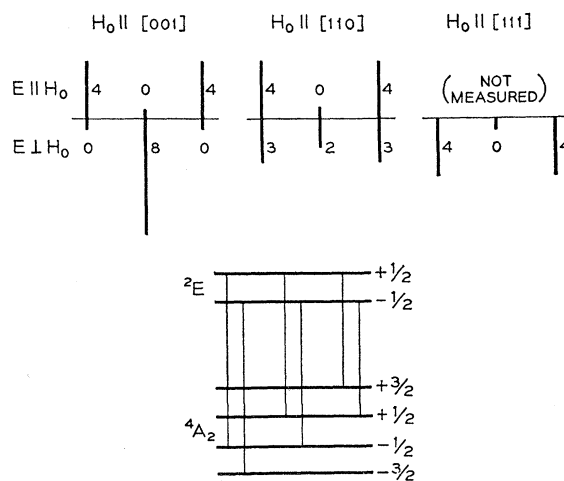
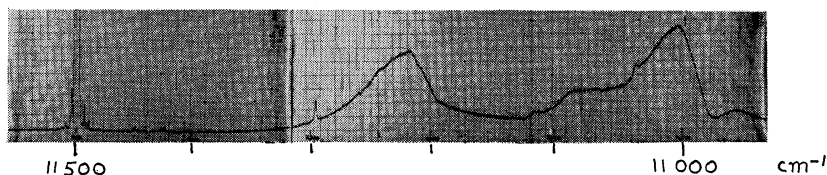


FIG. 2. Normalized experimental intensities of the Zeeman components of the 11 498  $\text{cm}^{-1}$  fluorescence, with the magnetic field in different crystallographic directions. The numbers represent the theoretical relative intensities assuming pure magnetic dipole transitions.

FIG. 3. Fluorescence of MgO:V<sup>2+</sup> (Conc. ~0.1% V<sup>2+</sup>) at 77°K, 10 950–11 550 cm<sup>-1</sup>.



The angular variation of the Zeeman pattern is shown in Fig. 5. Each component is labeled with its predominant polarization near  $\theta=0^\circ$ . The experimental points and fitted theoretical curves are shown. The calculations of Schulz-duBois<sup>13</sup> are used to find the Zeeman levels of the ground state. The upper states are assumed to be split according to the usual formula for a Kramers doublet

$$g^2 = g_{11}^2 \cos^2\theta + g_1^2 \sin^2\theta.$$

The fitted  $g$  values are given in Table I. The theoretical values are calculated with the program of Sugano and Peter,<sup>7</sup> using the following values for the parameters

TABLE I. Zero-field splittings and  $g$  values in Al<sub>2</sub>O<sub>3</sub>:V<sup>2+</sup>.

State	$g_{11}$		$g_1$		Splitting (cm <sup>-1</sup> )	
	Obs	Calc	Obs	Calc	Obs	Calc
<sup>4</sup> A <sub>2</sub>	1.99±0.01	1.99±0.01	0.33±0.02	0.07	12.35±0.03	12.1
$\bar{E}$	2.22±0.02	2.22	0.0 ±0.1	0.005	0.33±0.02	0.07
2 $\bar{A}$	1.61±0.03	1.60	0.0 ±0.1	0.08		

(see Sec. 4):  $K = -140$  cm<sup>-1</sup>,  $\zeta = 140$  cm<sup>-1</sup>,  $k = 0.55$ ,  $\epsilon = 0$ . A slightly better fit to the R1 pattern can be obtained by taking  $g_1 = 0.05$  for the  $\bar{E}$  state, but the difference is probably not significant (as it could be caused by a slight misorientation of the specimen). The observed polarizations agree qualitatively with those predicted<sup>6</sup> but are only about 70% complete.

The fluorescent lifetime of both states is about 70 msec at 77°K and 30 msec at 300°K. The lifetime at 77° is surprisingly long compared with that in ruby (4 msec)

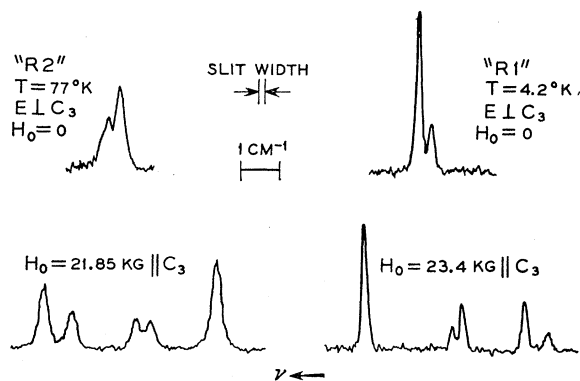


FIG. 4. Zero-field intensities and Zeeman effect of the 11 679 cm<sup>-1</sup> (R1) and 11 691 cm<sup>-1</sup> (R2) fluorescence of Al<sub>2</sub>O<sub>3</sub>:V<sup>2+</sup>.

<sup>13</sup> E. O. Schulz-duBois, Bell System Tech. J. 38, 271 (1959).

and in manganese corundum (0.8 msec).<sup>8</sup> It puts an upper limit of  $3 \times 10^{-8}$  on the oscillator strength of the transition from each upper level (assuming unit quantum efficiency),<sup>14</sup> compared with  $3 \times 10^{-7}$  for ruby, and  $3 \times 10^{-7}$  for Mn<sup>4+</sup>. The long lifetime and narrow linewidth of this transition suggest its use in an optical maser. So far, however, it has not been possible to obtain sufficient concentration of V<sup>2+</sup> in corundum to give a useful gain.

### C. Absorption and Excitation Spectra in MgO and Al<sub>2</sub>O<sub>3</sub>

The visible and near infrared absorption of vanadium doped magnesium oxide, before and after heating in hydrogen, is shown in Fig. 6. The absorption before heat treatment is entirely due to V<sup>3+</sup>, except for a broad absorption band in the region of 10 500 cm<sup>-1</sup>, which is

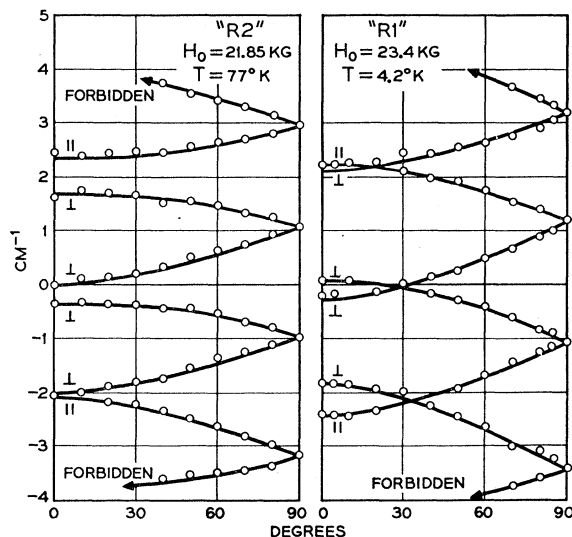


FIG. 5. Angular variation of the Zeeman effect of the R1 and R2 lines in Al<sub>2</sub>O<sub>3</sub>:V<sup>2+</sup>.

<sup>14</sup> Oscillator strengths are calculated from the following formulas [D. R. Dexter, in *Solid State Physics*, edited by F. Seitz and D. Turnbull (Academic Press Inc., New York, 1958), Vol. 6, p. 360]:

$$\int \sigma d\nu = \left( \frac{E_{\text{eff}}}{E_0} \right)^2 \frac{\pi e^2}{n m c^2} f,$$

$$\tau^{-1} = 8\pi^2 c n^2 \nu^2 \int \sigma d\nu.$$

Here  $\sigma$  is the absorption cross section per ion in cm<sup>2</sup>,  $\nu$  is the frequency in cm<sup>-1</sup>,  $n$  is the refractive index, and  $E_{\text{eff}}/E_0 = 1 + (n^2 - 1)/3$  for a tightly bound center in a cubic environment.

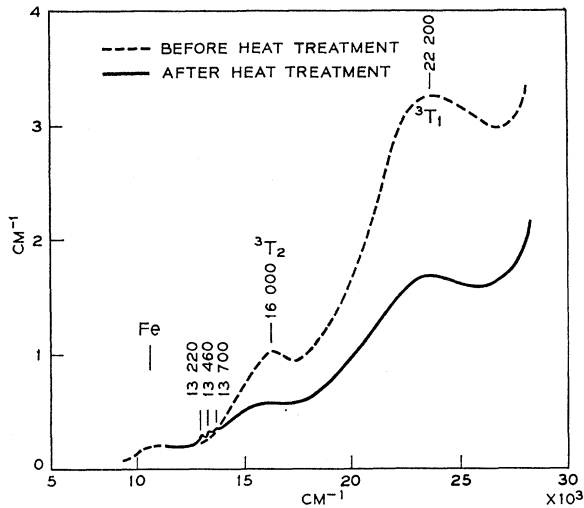


FIG. 6. Absorption of MgO:V (Conc.  $\sim 0.1\%$  V) before and after heating in  $H_2$  at  $1200^\circ C$ .

attributed to  $Fe^{2+}$ , as there is  $0.04\%$  iron in the sample. The assignments of the  $V^{3+}$  bands are shown, corresponding to those previously observed in vanadium corundum.<sup>15</sup> The effect of heat treatment is to reduce the amount of  $V^{3+}$  by about  $50\%$ , but the only sign of additional optical absorption which could be attributed to  $V^{2+}$  is the small group of three peaks starting at  $13\,220\text{ cm}^{-1}$ , of intensity about  $0.03\text{ cm}^{-1}$ . The oscillator strength of the  $13\,220\text{ cm}^{-1}$  peak is about  $2 \times 10^{-7}$ . This is just what one would calculate on the assumption of a pure magnetic dipole transition.<sup>3</sup>

The absorption of vanadium corundum is always entirely due to  $V^{3+}$ , except that in the most heavily irradiated specimens a broad very weak band appears at about  $14\,000\text{ cm}^{-1}$ . It is not polarized, as the bands in this region of the excitation spectra are (see below), and I do not believe it to be due to  $V^{2+}$ .

It appears that at the concentrations so far obtained the absorption spectra will be of little use in determining the energy levels of  $V^{2+}$ . Instead we turn to the excitation spectra.<sup>16</sup> The excitation spectrum of the  $11\,498\text{ cm}^{-1}$  fluorescence of heat treated magnesium oxide is shown in Fig. 7. Two sections of the spectrum are shown on an expanded vertical scale. The assumption will be made that the peaks in the excitation spectrum correspond in position to peaks in the absorption spectrum of the  $V^{2+}$  ion. That no energy transfer from  $V^{3+}$  is occurring is shown by the absence of excitation at  $22\,200\text{ cm}^{-1}$ , where  $V^{3+}$  has an absorption peak. The good agreement between the peaks in the excitation spectrum at  $13\,200$ ,  $13\,435$ , and  $13\,675\text{ cm}^{-1}$  with those in the absorption spectrum (the difference being within the calibration error) supports the assumption. In principle a correction should be made to the excitation spectrum to allow for competitive absorption by  $V^{3+}$ . However, the correction to the position of sharp peaks will be small, while the maxima of broad bands cannot be located precisely anyway, so such a correction has not been made. No significance can be attached to the relative intensities of the peaks, as not only are they strongly affected by the  $V^{3+}$  absorption but also quantum efficiency varies with the exciting wavelength. The very weak maxima in the region  $11\,700\text{--}12\,400\text{ cm}^{-1}$

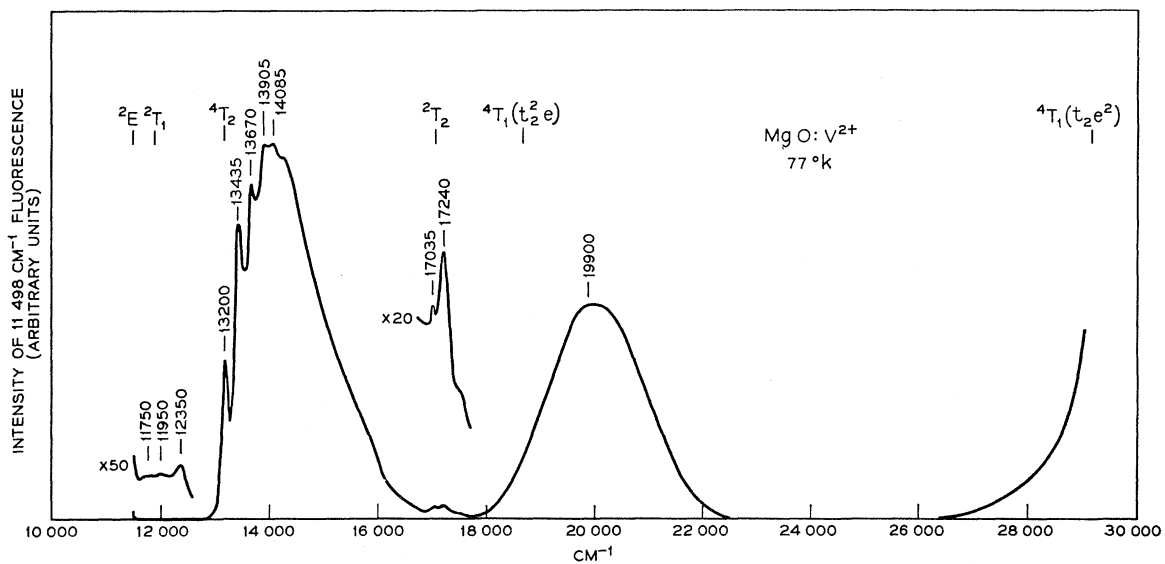
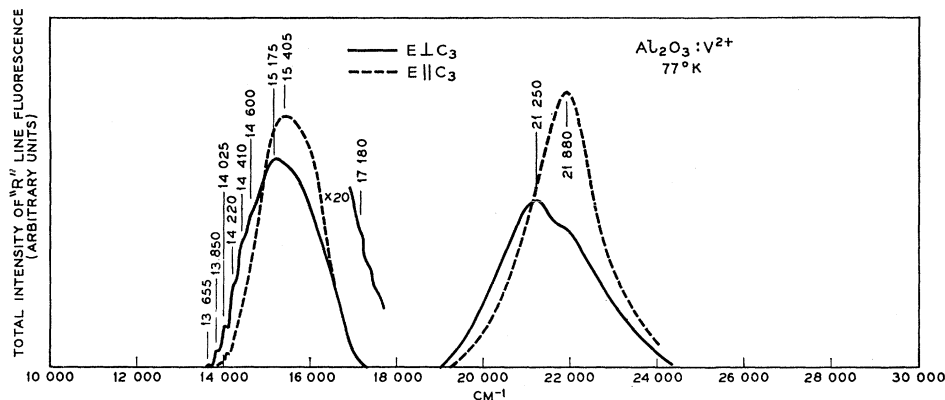


FIG. 7. Excitation spectrum of the  $11\,498\text{ cm}^{-1}$  fluorescence of MgO: $V^{2+}$  at  $77^\circ K$ . Spectral slit width  $50\text{--}70\text{ cm}^{-1}$ . The very weak lines in the  $12\,000\text{ cm}^{-1}$  region could be spurious. The theoretical cubic field levels are marked.

<sup>15</sup> M. H. L. Pryce and W. A. Runciman, *Discussions Faraday Soc.* **26**, 34 (1958).

<sup>16</sup> The excitation spectrum of a fluorescent center is the function  $I(\gamma, \gamma_0)$ , where  $I$  is the intensity of fluorescence emitted at the fixed frequency  $\gamma_0$  when the center is excited by the variable frequency  $\gamma$ .

FIG. 8. Excitation spectrum of the total  $R$  line fluorescence of  $\text{Al}_2\text{O}_3:\text{V}^{2+}$  at  $77^\circ\text{K}$ . The structure in  $\pi$  polarization in the  $13\,900\text{ cm}^{-1}$  region is rather uncertain.



were observed with a spectral slit width of  $150\text{ cm}^{-1}$ . Even then they were barely detectable above noise and may be spurious.

The polarized excitation spectrum of the total " $R$ " line fluorescence of  $\text{V}^{2+}$  in corundum is shown in Fig. 8. The polarization of the fluorescence was not studied. The results are not as good as those for magnesium oxide, as the fluorescence is very much weaker. Two weak maxima in  $\pi$  polarization at  $13\,860$  and  $14\,045\text{ cm}^{-1}$  may be due to imperfect polarization. Apart from these, no vibrational structure is observed in  $\pi$  polarization. The great strength of the  $\pi$ -polarized vibrational maximum at  $15\,405\text{ cm}^{-1}$  relative to the  $\sigma$ -polarized maximum at  $15\,175\text{ cm}^{-1}$  is difficult to understand; we would expect by analogy with ruby (and according to theory<sup>6</sup>) that the  $\pi$  absorption band would be much weaker than the  $\sigma$  band.

#### 4. DISCUSSION

##### A. Assignments and Vibrational Structure

In order to assign many of the observed peaks in the excitation spectrum to their respective electronic transitions, the vibrational structure associated with these transitions must be understood. Unfortunately, data on the infrared and Raman spectra of magnesium oxide are rather contradictory and incomplete. The longitudinal and transverse Raman frequencies appear to be in the regions  $580\text{--}620\text{ cm}^{-1}$  and  $350\text{--}400\text{ cm}^{-1}$ , respectively.<sup>17,18</sup> There is some indication in the infrared spectrum of a peak in the phonon density of states (presumably where an acoustic branch meets the zone boundary) in the region of  $250\text{ cm}^{-1}$ .

The vibrational structure observed in fluorescence (Fig. 3) has the general appearance of a phonon density of states curve. The peaks at  $270$  and  $540\text{ cm}^{-1}$  could be attributed to the emission of one and two acoustic phonons, respectively; that at  $490\text{ cm}^{-1}$  to the emission of an optical phonon. These phonons will be predominantly near the zone boundary, because of the

great density of states there, the momentum selection rule having been destroyed by the presence of the impurity. The structure observed in the excitation spectrum can be treated in the same way.<sup>19</sup> I, therefore, tentatively assign the  $11\,750$  and  $11\,950\text{ cm}^{-1}$  peaks to the  ${}^4A_2 \rightarrow {}^2E$  transition with the emission of a single phonon. The  $13\,200\text{ cm}^{-1}$  peak is presumably the pure electronic  ${}^4A_2 \rightarrow {}^4T_2$  transition, and the  $13\,435$  and  $13\,670\text{ cm}^{-1}$  peaks correspond to the emission of a single phonon; subsequent peaks involve the emission of two or more phonons. The peaks at  $17\,035$  and  $17\,240\text{ cm}^{-1}$  correspond to the  ${}^4A_2 \rightarrow {}^2T_2$  transition, most probably with the emission respectively of a  $270$  and  $490\text{ cm}^{-1}$  phonon; the pure electronic transition would then be at  $16\,750\text{ cm}^{-1}$ , and being both spin and parity forbidden is too weak to be seen. Similarly the  $12\,350\text{ cm}^{-1}$  peak is probably the  ${}^4A_2 \rightarrow {}^2T_1$  phonon assisted transition, the pure electronic transition is tentatively put at  $11\,860\text{ cm}^{-1}$ . The  $19\,900\text{ cm}^{-1}$  band corresponds to the  ${}^4A_2 \rightarrow {}^4T_1$  ( $t_2^2e$ ) transition accompanied by a large number of emitted phonons; similarly the rise towards  $30\,000\text{ cm}^{-1}$  is due to the  ${}^4A_2 \rightarrow {}^4T_1$  ( $t_2e^2$ ) transition. These assignments agree well with the theoretical energy levels which will be derived in the next section and are marked in Fig. 7.

The vibrational structure in the case of corundum is much less clear-cut; but assignments of the cubic field states can be made by analogy with magnesium oxide, and the trigonal field splittings (when observed) are qualitatively similar to those of ruby. As in ruby, the vibrational structure of the  ${}^4T_2$  band is much weaker in  $\pi$  polarization than in  $\sigma$ . This point is discussed by McClure.<sup>20</sup>

The observed energy levels are collected in Table II. The first column labels the states according to their

<sup>17</sup> S. J. Khambata, Proc. Phys. Soc. (London) **A69**, 426 (1956).

<sup>18</sup> J. C. Willmott, Proc. Phys. Soc. (London) **A63**, 389 (1950).

<sup>19</sup> The structure observed in the absorption spectrum of  $\text{Co}^{2+}$  in  $\text{MgO}$  [R. Pappalardo, D. L. Wood, and R. C. Linares, J. Chem. Phys. **35**, 2041 (1961)] and in the fluorescence and absorption spectra of  $\text{Ni}^{2+}$  in  $\text{MgO}$  [F. A. Kroger, H. J. Vink, and J. Van den Boomgaard, Physica **18**, 77, 1952; R. Pappalardo, D. L. Wood, and R. C. Linares, J. Chem. Phys. **35**, 1460 (1961)] is consistent with this picture, but the frequencies are slightly lower, apparently being perturbed by the presence of the impurity.

<sup>20</sup> D. S. McClure, J. Chem. Phys. **36**, 2757 (1962).

TABLE II. Spectrum of  $V^{2+}$  in octahedral coordination.

$O_h$ repn.	MgO:V <sup>2+</sup> Obs		Al <sub>2</sub> O <sub>3</sub> :V <sup>2+</sup>				Pol.
	Pure (cm <sup>-1</sup> )	Vib. (cm <sup>-1</sup> )	Calc (cm <sup>-1</sup> )	$C_3$ repn.	Pure (cm <sup>-1</sup> )	Vib. (cm <sup>-1</sup> )	
$^4A_2$	0		0		$M_s = \pm\frac{3}{2} - 0.165$		
					$M_s = \pm\frac{1}{2} + 0.165$		
$^2E$	11 498.6	11 750 11 950	11 450		$\bar{E}$ 11 679.15 $2\bar{A}$ 11 691.5		$\sigma$ $\sigma$
$^2T_1$	(11 860?)	12 350	11 900				
$^4T_2$	13 200	13 435 13 670 13 905 14 085	13 200	$^4E$	13 655	13 850 14 025 14 220 14 410 14 600 (15 175)	$\sigma$ $\sigma$ $\sigma$ $\sigma$ $\sigma$ $\pi$
				$^4A_1$	13 860?	14 045? (15 405)	
$^2T_2$	(16 760)	17 035 17 240 (19 900)	17 100	?		17 160	$\pi$
$^4T_1(^4z^2e)$		(19 900)	18 700	$^4E$		(21 250)	$\sigma$
$^4T_1(^4ze^2)$		(~30 000)	29 200	$^4A_2$		(21 880)	$\pi$

representations in the  $O_h$  group, the fifth according to those in the  $C_3$  group (in the mixed notation of Sugano and Tanabe<sup>6</sup>). The second column gives the frequencies of the pure electronic transitions of  $V^{2+}$  in magnesium oxide; those in brackets were not observed directly but deduced from the vibrational structure. The third column gives the frequencies of the vibrational peaks, those in brackets being broad maxima in which the individual vibrational peaks are not resolved. The fourth column gives the theoretical position of the pure electronic lines in a cubic field,<sup>5</sup> calculated in the next section. The sixth and seventh columns give, respectively, the pure electronic lines and the vibrational peaks for  $V^{2+}$  in corundum. The last column gives the theoretical polarization of the transition from the ground state.<sup>6</sup>

## B. Determination of the Crystal Field Parameters

We begin by analyzing the spectrum in terms of Tanabe and Sugano's calculations.<sup>5,6</sup> These proceed in two stages. First, the energy matrices for the  $d^3$  configuration in a cubic field are set up in a strong field representation and solved rigorously (spin-orbit coupling is neglected). Then the splitting of each cubic field level of interest by spin-orbit coupling, noncubic crystal fields, and by an external magnetic field, is calculated by perturbation theory. Interaction between states of different strong cubic field configuration is neglected. Certain points of the spectrum cannot be dealt with by this method as they depend on this configuration interaction; this problem is treated by Sugano and Peter.<sup>7</sup> The advantage of the perturbation theory approach is that formulas can be found for most of the experimental quantities which are simple, even if only approximate.

We first consider the levels in a cubic field and neglect covalency effects except insofar as the parame-

ters differ from their free-ion values. The "calculated" levels in Table II were found from Tanabe and Sugano's<sup>6</sup> matrices with the following parameters:  $Dq = 1320$  cm<sup>-1</sup>,  $B = 550$  cm<sup>-1</sup>,  $C/B = 4.5$ .  $Dq$  is the cubic field parameter,  $B$  and  $C$  the Racah parameters describing the electrostatic interaction between the three  $d$  electrons.  $C/B$  is taken to have its free-ion value, so there are effectively only two adjustable parameters. The agreement is excellent.

In a trigonally distorted octahedral field the  $^2E$  state is split by an amount  $\lambda$ . Perturbation theory gives<sup>6</sup>

$$\lambda = 4K\zeta / [W(^2T_2) - W(^2E)],$$

and for the  $g$  factors of the two states

$$g_{11}(2\bar{A}) = g_1 - 2g_2, \quad g_{11}(\bar{E}) = g_1 + 2g_2,$$

$$g_1 = 2 - 8k\zeta K / [W(^2T_2) - W(^2E)][W(^2T_1) - W(^2E)],$$

$$g_2 = 12kK^2 / [W(^2T_2) - W(^2E)][W(^2T_1) - W(^2E)] + 6kK^2 / [W(^2T_2) - W(^2E)]^2.$$

Here  $W(\Gamma)$  is the energy of the cubic field state  $\Gamma$ , and  $\zeta$ ,  $K$ , and  $k$  are the expectation values over the  $t_2$  manifold of the spin-orbit coupling, trigonal field, and angular momentum, respectively.

$W(^2T_2) \gg W(^2T_1)$  so the second term in the formula for  $g_2$  can be neglected. From the experimental values  $g_1 = 1.915 \pm 0.02$ ,  $g_2 = 0.15 \pm 0.01$ ,  $\lambda = 12.35$  cm<sup>-1</sup>,  $W(^2T_2) - W(^2E) = 5500$  cm<sup>-1</sup>, we find  $K = -140 \pm 20$  cm<sup>-1</sup>,  $\zeta = 120 \pm 15$  cm<sup>-1</sup>,  $[W(^2T_1) - W(^2E)]/k = 290 \pm 70$  cm<sup>-1</sup>. If the assignment of the  $^2T_1$  state as 11 860 cm<sup>-1</sup> is correct, we find formally  $k = 1.3 \pm 0.3$ . As the maximum possible value of  $k$  is unity, the present approach appears to be inadequate, and configuration interaction must be taken into account in determining the  $g$  values.

This has been done for ruby by Sugano and Peter,<sup>7</sup> and I have used their program to fit the spectrum of  $V^{2+}$ . Good agreement can be obtained (see Table I) if we take  $K = 140$  cm<sup>-1</sup>,  $\zeta = 140$  cm<sup>-1</sup>,  $k = 0.55$ . (The parameter  $\epsilon$ , which measures the difference in covalency between the  $t_2$  and  $e$  orbitals, was arbitrarily taken as zero to decrease the number of adjustable parameters.) As we don't have the data on the  $^2T_2$  state to provide a check on these values of the parameters, they must be taken as rather tentative. Sugano and Peter found that in order to fit approximately all the data for  $Cr^{3+}$  it is necessary to tolerate values of  $2-g_1$  and  $g_2$  for the  $^2E$  states which are rather greater than the experimental values. A similar deviation in the case of  $V^{2+}$  would lead to larger values of  $K$  and  $k$  and a smaller value of  $\zeta$ . Reasonable values for these would be  $K \sim 160$  cm<sup>-1</sup>,  $\zeta \sim 110$  cm<sup>-1</sup>,  $k \sim 0.65$ .

The  $g$  value of the  $^2E$  state in a cubic field is 2 according to Sugano and Tanabe's formulas. Sugano and Peter's calculation, with the same values of  $\zeta$  and  $k$ , but putting  $K = 0$ , gives  $g = 1.89$ , in excellent agreement with the experimental values in magnesium oxide of 1.88.

TABLE III. Oscillator strengths and ground-state splittings of  $3d^3$  ions in  $\text{Al}_2\text{O}_3$ .

Ion	$10^7 f(R_1)$	$[W(^4T_2) - W(^2E)]^2 f/\nu$ ( $10^{-9} \text{ cm}^{-1}$ )	$-2D$ ( $\text{cm}^{-1}$ )
$\text{V}^{2+}$	$\leq 0.3$	$< 1.1$	0.33
$\text{Cr}^{3+}$	3	11.5	0.38
$\text{Mn}^{4+}$	$\sim 3$	$\sim 35$	0.39

According to Sugano and Tanabe the  $^4T_2$  and  $^4T_1$  states should be split in first order by the trigonal field, the splitting in both cases being  $\frac{2}{3}K$ . This is borne out by Sugano and Peter's calculation [which, however, neglects interaction with the  $^4T_1(t_2e^2)$  state]. The splitting of the  $^4T_2$  state, 205 or 235  $\text{cm}^{-1}$ , is consistent with this predicted value of 210  $\text{cm}^{-1}$ . On the other hand, the splitting of the  $^4T_1$  band is 630  $\text{cm}^{-1}$ . This discrepancy, which is also observed in ruby,<sup>20</sup> may not be due to a failure of the theory for the electronic states, but to the fact that the different trigonal field states interact differently with the crystal vibrations, so that the separation of the vibrational maximum from the pure electronic line is different for the different polarizations.

The splitting of the  $^4A_2$  ground state in corundum is much larger than predicted by Sugano and Peter's calculation with any reasonable values of the parameters (see Table I). Two alternative explanations of the ground-state splitting have been put forward. Artman and Murphy<sup>21</sup> have shown that the ground state of a  $d^3$  ion located at a site without a center of symmetry is split by the hemihedral crystal field. They argue that a hemihedral field of the right order of magnitude to explain the oscillator strength of the crystal field transitions in ruby will also explain the magnitude of the ground state splitting. The oscillator strength  $f$  of an  $R$  line is proportional to  $\nu^2 |P|^2 / [W(^4T_2) - W(^2E)]^2$ , where  $|P|$  is proportional to the hemihedral field  $V_{\text{hem}}$ . In the theory of Artman and Murphy the ground-state splitting  $2D$  is proportional to  $(\zeta V_{\text{hem}})^2$ . We would, therefore, expect  $2D$  to vary as  $[W(^4T_2) - W(^2E)]^2 f/\nu$ . Table III demonstrates that this is far from the truth. Kamimura<sup>22</sup> has pointed out that the ground-state splitting and anisotropy of the  $g$  factor in ruby can be explained by assuming the spin-orbit coupling to be about 15% anisotropic on account of covalency effects. A similar degree of anisotropy would explain the ground-state splittings of  $\text{V}^{2+}$  and  $\text{Mn}^{4+}$ , but in the absence of accurate  $g$  values for  $\text{V}^{2+}$  no conclusion can be drawn at present.

### C. The Values of the Crystal Field Parameters

The parameters used to describe the spectra of the isoelectronic  $d^3$  sequence  $\text{V}^{2+}$ ,  $\text{Cr}^{3+}$ ,  $\text{Mn}^{4+}$  in corundum

TABLE IV. Crystal-field and Free-ion parameters for  $3d^3$  ions in  $\text{Al}_2\text{O}_3$ . (1 a.u. = 0.53 Å.)

	$r_G$ (au)	$\langle r \rangle$ (au)	$\langle r^2 \rangle$ ( $\text{au}^2$ )	$\langle r^4 \rangle$ ( $\text{au}^4$ )	$Dq$ ( $\text{cm}^{-1}$ )	$B/B_0$	$\zeta/\zeta_0$	$k$	$-K$ ( $\text{cm}^{-1}$ )
$\text{V}^{2+}$ (a)	1.36	1.28	2.06	9.50	1360	0.73	0.83	0.55	140
(b)									
$\text{Cr}^{3+}$	1.23	1.08	1.45	4.45	1670	0.76	0.62	0.62	330
$\text{Mn}^{4+}$	0.98	0.97	1.11	2.39	2100	0.66			700
$\text{Al}^{3+}$	0.96								
$\text{Mg}^{2+}$	1.25								

are collected in Table IV. The subscript 0 indicates the free-ion values (taken from references 4 and 5). The parameters for  $\text{Cr}^{3+}$  were determined by Sugano and Peter.<sup>7</sup> Those for  $\text{Mn}^{4+}$  were determined by Geschwind *et al.*<sup>8</sup> and are very tentative, particularly the value of  $K$ . The two sets of parameters for  $\text{V}^{2+}$  are (a) those obtained by a strict fit to the  $^2E$  state results, and (b) those guessed at in the previous section as being more reasonable. Also given are the Goldschmidt radii  $r_G$ , and the averages  $\langle r \rangle$ ,  $\langle r^2 \rangle$ , and  $\langle r^4 \rangle$  over the  $d$  shell of the free ion, derived from the wave functions calculated by Watson.<sup>23</sup>

Two qualitative observations can be made. The covalency of  $\text{V}^{2+}$  as measured by  $B/B_0$ ,  $\zeta/\zeta_0$ , and  $k$  is about the same as that of  $\text{Cr}^{3+}$ , in spite of the fact that  $\text{V}^{2+}$  is a tighter squeeze in an  $\text{Al}^{3+}$  site. On the other hand, the change in  $Dq$  in going from  $\text{V}^{2+}$  to  $\text{Cr}^{3+}$  is less than that usually observed in going from a divalent to a trivalent ion. The covalency of  $\text{Mn}^{4+}$  is much greater,<sup>8</sup> presumably because the  $3d$  wave function is hardly screened at all by the  $3s$  (whose extent is indicated by the Goldschmidt radius). Secondly, it is possible to explain qualitatively the trend in the trigonal field parameter  $K$  along the lines suggested by McClure.<sup>20</sup> He uses the point charge model for trivalent transition ions in corundum, and can explain the sign and order of magnitude of  $K$  if he assumes the impurity ion to be displaced from the  $\text{Al}^{3+}$  site about 0.1 Å towards the empty octahedral site. This is consistent with the fact that the transition ions are larger than the  $\text{Al}^{3+}$  ions they replace. Rather than calculate the averages  $\langle r^n \rangle$  from the free-ion wave functions, he treats them as adjustable parameters. As he only considers trivalent impurity ions, he can reasonably neglect displacements of the oxygen ions, but if we are to extend his treatment to ions of different valency from those they replace, we must take such displacements into account. If we assume as a first approximation that the oxygen ions are only displaced radially, the major effect on the crystal field parameters will be equivalent to a change of linear scale. Further, let us assume that the effect of covalency is also to alter the linear scale of the wave function without altering its shape. For an impurity ion displaced 0.1 Å towards the empty octahedral site

<sup>21</sup> J. O. Artman and J. C. Murphy, Bull. Am. Phys. Soc. 7, 196 (1962).

<sup>22</sup> H. Kamimura, Phys. Rev. 128, 1077 (1962).

<sup>23</sup> R. E. Watson, Solid State and Molecular Theory Group, Massachusetts Institute of Technology, Technical Report No. 12, 1959 (unpublished).

McClure gives

$$Dq = 106\langle r^4 \rangle,$$

$$K = -\frac{1}{3}v = 302\langle r^2 \rangle - 68\langle r^4 \rangle.$$

Here,  $K$  and  $Dq$  are in  $\text{cm}^{-1}$ ,  $r$  is in atomic units (au), the charge on the oxygen ions in  $-2e$  and the numerical coefficients are those calculated for the normal oxygen positions, any variation being taken up in the  $\langle r^n \rangle$ . Following McClure, we determine an effective average  $\langle r^4 \rangle_{\text{eff}}$  from  $Dq$ . If we now assume Watson's Hartree-Fock wave function<sup>23</sup> to be radially expanded by a scale factor  $\rho$ , where  $\rho^4 = \langle r^4 \rangle_{\text{eff}} / \langle r^4 \rangle_{H-F}$ , we can calculate  $\langle r^2 \rangle_{\text{eff}} = \rho^2 \langle r^2 \rangle_{H-F}$ . Finally, we substitute the new  $\langle r^n \rangle_{\text{eff}}$  in the formula for  $K$ . The results are given in Table V; Table V shows the correct trend in  $K$ , though no significance can be attached to exact values, particularly as  $K$  is rather sensitive to the position of the ion on the  $C_3$  axis, which we have assumed to be fixed. Note that the model requires the  $\text{Mn}^{4+}$  ion to be (effectively) larger than the  $\text{V}^{2+}$  ion, whereas the free ion is, of course, smaller and if we had used the free-ion values of  $\langle r^n \rangle$  the trend in  $K$  would have been in the opposite direction. This discrepancy is illustrative of the heuristic nature of the model.

TABLE V. Point-charge calculation of  $K$ .

Ion	$\langle r^4 \rangle_{\text{eff}}$ (au <sup>4</sup> )	$\rho$	$\langle r^2 \rangle_{\text{eff}}$ (au <sup>2</sup> )	$-K(\text{calc})$ (cm <sup>-1</sup> )	$-K(\text{obs})$ (cm <sup>-1</sup> )
$\text{V}^{2+}$	12.8	1.08	2.4	140	150
$\text{Cr}^{3+}$	15.7	1.37	2.7	260	330
$\text{Mn}^{4+}$	19.8	1.70	3.2	400	700

## 5. CONCLUSIONS

Four main points have been made. First, a great deal of information about a fluorescent center can be obtained from its excitation spectrum, even when the absorption spectrum is too weak to be observed. Second, in discussing the vibrational structure associated with electronic transitions, the possibility of interaction with phonons away from the center of the Brillouin zone must be taken into account. As a phonon has the full crystal symmetry only when it is at the zone center, selection rules dependent on that symmetry will in general be violated. Third, the large variation in oscillator strength of  $d^3$  ions in corundum while the ground-state splitting remains relatively constant is prima facie evidence that the hemihedral part of the crystal field is not responsible for the splitting, at any rate in  $\text{V}^{2+}$ . Finally, the trigonal field parameter changes through the isoelectronic sequence in a way that is consistent with McClure's formulation of the point-charge model.

## ACKNOWLEDGMENTS

My thanks are due to A. Yariv for making the quantitative spin resonance measurements, to F. H. Doleiden and Miss D. M. Dodd for taking the absorption spectra, to Miss B. B. Cetlin for letting me use her program for the Sugano and Peter calculation, and to J. A. Ditzemberger for technical assistance. I am also grateful to A. L. Schawlow, P. Auzins, H. Kamimura, S. Geschwind, M. Peter, G. E. Devlin, W. M. Augustyniak, and J. Ferguson for helpful discussions.



FIG. 3. Fluorescence of MgO:V<sup>2+</sup>  
(Conc. ~0.1% V<sup>2+</sup>) at 77°K, 10 950-  
11 550 cm<sup>-1</sup>.

